

# Discovery reach for non-standard interactions in a neutrino factory

Joachim Kopp,<sup>a</sup> Manfred Lindner,<sup>b</sup> and Toshihiko Ota<sup>c</sup>

*Max-Planck-Institut für Kernphysik,  
Postfach 10 39 80, 69029 Heidelberg, Germany*

We study the discovery reach for Non-Standard Interactions (NSIs) in a neutrino factory experiment. After giving a theoretical, but model-independent, overview of the most relevant classes of NSIs, we present detailed numerical results for some of them. Our simulations take into account matter effects, uncertainties in the neutrino oscillation parameters, systematical errors, parameter correlations, and degeneracies. We perform scans of the parameter space, and show that a neutrino factory has excellent prospects of detecting NSIs originating from new physics at around 1 TeV, which is a scale favored by many extensions of the standard model. It will also turn out that the discovery reach depends strongly on the standard and non-standard CP violating phases in the Lagrangian.

PACS numbers: 13.15.+g, 14.60.Pq, 12.60.-i

## 1. INTRODUCTION

Huge efforts are currently undertaken to design new long-baseline neutrino experiments to precisely measure the three-flavor oscillation parameters, in particular the yet unknown mixing angle  $\theta_{13}$ , the CP violating phase  $\delta_{\text{CP}}$ , and the sign of the atmospheric mass squared difference  $\Delta m_{31}^2$ . However, the excellent accuracy with which the planned setups can measure the oscillation probabilities, will also allow for the detection of new sub-leading effects, such as mixing with sterile neutrinos, a non-unitary Pontecorvo-Maki-Nakagawa-Sakata (PMNS) matrix, neutrino decay, the decoherence effect, CPT violation, or mass-varying neutrinos. Furthermore, many extensions of the standard model predict new, effective four-Fermi interactions involving neutrinos, on which we will focus in this paper. General phenomenological studies of these non-standard interactions (NSIs) have been conducted in [1, 2, 3, 4, 5, 6, 7, 8], and specific models are discussed in [9, 10]. After a work by Grossman [11], which pointed out the importance of NSIs for neutrino oscillation experiments, many authors have investigated their impact in the context of solar neutrinos [12, 13, 14, 15], atmospheric neutrinos [16, 17, 18, 19, 20, 21], conventional and upgraded neutrino beams [22, 23, 24, 25, 26, 27, 28], neutrino factories [8, 23, 29, 30, 31, 32, 33, 34], beta beams [35], supernova neutrinos [36, 37], cosmological relic neutrinos [38],  $e^+e^-$  colliders [39], neutrino-electron scattering [40], and neutrino-nucleus scattering [41, 42]. Existing experimental bounds are presented in [43].

In this article, we will discuss in particular the discovery potential of a neutrino factory [44, 45, 46, 47, 48, 49, 50], which is currently the most advanced tech-

nology discussed in neutrino physics, and would have a precision of  $\mathcal{O}(1\text{--}0.1)\%$  on some of the oscillation probabilities. We will show that this translates into a sensitivity to NSIs originating from scales of up to several TeV. We will focus only on non-standard interactions (NSIs) which violate lepton flavor. Existence of such interactions would typically induce not only effects in the neutrino sector, but also charged lepton flavor violating processes like  $\mu \rightarrow 3e$ . However, in the charged lepton sector, the signal is proportional to the *square* of the non-standard coupling, while in an oscillation experiment, interference between the standard and non-standard amplitudes will also induce terms which are linear in the coupling constant and can therefore be expected to be easier to detect.

A long baseline neutrino oscillation experiment consists of three stages: beam production (source), beam propagation through the Earth, and neutrino detection at the far site. Here, we are going to consider NSIs which modify only one of these aspects at a time. In principle, there may also exist combined effects of several new processes, but these will be suppressed by higher powers of the small coupling constants.

The paper is organized as follows: In Sec. 2, we will describe the NSIs analytically, but in a model-independent way. Afterwards, in Sec. 3, we will present detailed numerical results on non-standard modifications to the neutrino production and propagation amplitudes. We have performed sophisticated simulations with a modified version of the GLoBES software [51, 52], taking into account systematical errors and correlations between all standard and non-standard oscillation parameters. Some of these correlations will turn out to be very strong, so our final results on the NSI discovery reach of a neutrino factory will strongly depend on the true parameter values. We will summarize our results in Sec. 4 and draw some conclusions.

<sup>a</sup>Email: jkopp@mpi-hd.mpg.de

<sup>b</sup>Email: lindner@mpi-hd.mpg.de

<sup>c</sup>Email: toshi@mpi-hd.mpg.de

## 2. NON-STANDARD INTERACTIONS IN NEUTRINO OSCILLATIONS

In the context of neutrino factory experiments, one usually considers the “golden oscillation channel”  $\nu_e \rightarrow \nu_\mu$ , the “silver channel”  $\nu_e \rightarrow \nu_\tau$ , the “platinum channel”  $\nu_\mu \rightarrow \nu_e$ , and the disappearance channel  $\nu_\mu \rightarrow \nu_\mu$  (see e.g. [47] and references therein). Of these, the golden channel is most important for the discovery of small effects such as  $\theta_{13}$ -oscillations, CP violation, but also non-standard interactions, because it is an appearance channel, and because it is technically more easily accessible than the silver and platinum channels. Therefore, we will focus on the golden channel and consider only NSIs influencing the corresponding process chain

$$\mu^+ \rightarrow \nu_e \xrightarrow{\text{Osc.}} \nu_\mu \rightarrow \mu^- . \quad (1)$$

NSIs can modify the production, oscillation, and detection of neutrinos, so that the following alternative processes to Eq. (1) can occur:

$$\mu^+ \xrightarrow{\text{NSI}} \nu_\mu \xrightarrow{\text{No osc.}} \nu_\mu \rightarrow \mu^- , \quad (2)$$

$$\mu^+ \rightarrow \nu_e \xrightarrow[\text{NSI}]{\text{No osc.}} \nu_\mu \rightarrow \mu^- , \quad (3)$$

$$\mu^+ \rightarrow \nu_e \xrightarrow{\text{No osc.}} \nu_e \xrightarrow{\text{NSI}} \mu^- . \quad (4)$$

These processes are illustrated diagrammatically in Fig. 1.

Since the initial and final states are the same in Eq. (1) and Eqs. (2) to (4), interference can occur on the level of the amplitudes [1, 2, 3, 4, 5, 11, 31]. This will enhance the magnitude of the new effects compared to scenarios where the NSIs are added non-coherently.

Non-standard interactions are typically generated by new physics at very high energy scales, so for a neutrino factory operating in the low-energy regime, they can be expressed as model-independent four-Fermi interactions:

$$\begin{aligned} \mathcal{L}_{\text{NSI}} = & \frac{G_F}{\sqrt{2}} \epsilon_{e\mu}^{s\mp} \{ \bar{\nu}_\mu \gamma^\rho (1 - \gamma^5) \nu_\mu \} \{ \bar{\mu} \gamma_\rho (1 \mp \gamma^5) e \} \\ & + \sum_{f=e,u,d} \frac{G_F}{\sqrt{2}} \epsilon_{e\mu}^{m,f\mp} \{ \bar{\nu}_e \gamma^\rho (1 - \gamma^5) \nu_\mu \} \{ \bar{f} \gamma_\rho (1 \mp \gamma^5) f \} \\ & + \frac{G_F}{\sqrt{2}} \epsilon_{e\mu}^{d\mp} \{ \bar{\mu} \gamma^\rho (1 - \gamma^5) \nu_e \} \{ \bar{u} \gamma_\rho (1 \mp \gamma^5) d \} + \text{h.c.} \end{aligned} \quad (5)$$

Here,  $G_F$  denotes the Fermi constant,  $\nu_e$  and  $\nu_\mu$  are the neutrino fields,  $e$  and  $\mu$  are the charged lepton fields, and  $u$ ,  $d$  are quark fields. Finally, the magnitude of the NSIs is parameterized by  $\epsilon_{e\mu}^{s\mp}$  for effects in the neutrino source, by  $\epsilon_{e\mu}^{m,f\mp}$  for non-standard matter effects on the oscillation, and by  $\epsilon_{e\mu}^{d\mp}$  for modifications to the detection process. In contrast to a previous study [31], we allow the  $\epsilon$  parameters to be complex. Then, Eq. (5) implies that the  $\epsilon$  parameters for anti-neutrino processes are the complex conjugates of those for neutrino processes.

The expected magnitude of the  $\epsilon$  parameters can be estimated as follows [29]: If we assume the non-standard interactions to arise at a scale  $M_{\text{NSI}}$ , the effective vertices in Eq. (5) will be suppressed by  $1/M_{\text{NSI}}^2$  in the same way as the standard weak interactions are suppressed by  $1/M_W^2$ . Therefore we expect

$$|\epsilon| \sim \frac{M_W^2}{M_{\text{NSI}}^2} . \quad (6)$$

The NSIs in the beam source, given by the first line of Eq. (5), effectively promote the initial neutrino state from a pure flavor eigenstate into the mixed state

$$|\nu_e^{(s)}\rangle = |\nu_e\rangle + \left\{ \epsilon_{e\mu}^{s-} + \epsilon_{e\mu}^{s+} \times \mathcal{O}\left(\frac{m_\mu m_e}{E_\mu E_e}\right) \right\} |\nu_\mu\rangle . \quad (7)$$

Similarly, the detector will project out the mixed state

$$\langle \nu_\mu^{(d)} | = \langle \nu_\mu | + \left\{ \epsilon_{e\mu}^{d-} + \epsilon_{e\mu}^{d+} \times \mathcal{O}\left(\frac{m_u m_d}{E_u E_d}\right) \right\} \langle \nu_e | \quad (8)$$

rather than the pure flavor eigenstate  $\langle \nu_\mu |$ . The kinematics of a neutrino factory experiment is such that in most regions of the phase space,  $E_{e,\mu,u,d} \gg m_{e,\mu,u,d}$ . This remains true even if we take into account that  $E_e$  and  $E_\mu$  as well as  $E_u$  and  $E_d$  are not independent, and if we allow  $E_u$  and  $E_d$  to be slightly off-shell due to QCD effects in the nucleus. We do not consider these hadronic effects here, but we remark that they will generally be soft compared to the primary neutrino interaction. Since interference of standard and non-standard processes can only occur if *all* initial and final state particles have the same chirality, it follows that the  $(V - A)(V + A)$  type NSIs are suppressed by the helicity factors  $\mathcal{O}(m_\mu m_e / E_\mu E_e)$  resp.  $\mathcal{O}(m_u m_d / E_u E_d)$ . Therefore, we will take

$$\epsilon_{e\mu}^s = \epsilon_{e\mu}^{s-} , \quad (9)$$

$$\epsilon_{e\mu}^d = \epsilon_{e\mu}^{d-} . \quad (10)$$

in the following.

Note that the  $\epsilon$  parameters do not necessarily form unitary matrices, so that the source and detection states, in general, do not form complete sets of basis vectors in the Hilbert space:

$$\sum_{\alpha=e,\mu,\tau} |\nu_\alpha^{(s)}\rangle \langle \nu_\alpha^{(s)}| \neq 1, \quad \sum_{\alpha=e,\mu,\tau} |\nu_\alpha^{(d)}\rangle \langle \nu_\alpha^{(d)}| \neq 1 . \quad (11)$$

However, we do require the PMNS matrix to be unitary, so that the standard mass and flavor eigenstates at least form a basis of the subspace of states participating in oscillations. Thus, the neutrino propagation does not violate unitarity, while the production and detection processes may do so. With these assumptions, neutrino oscillations can be described as usual by a hermitian  $3 \times 3$  Hamiltonian [31], that contains, however, an extra term

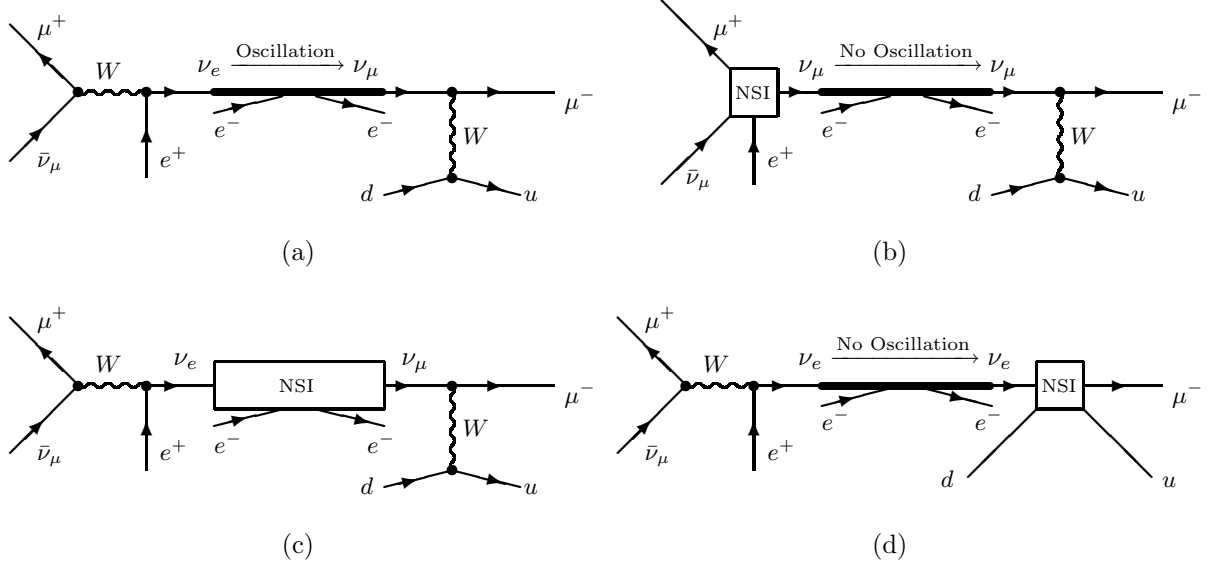


Figure 1: (a): The golden channel oscillation process in a neutrino factory (cf. Eq. (1)); (b) – (d): Non-standard contributions to the golden channel (cf. Eqs. (2) to (4)).

$H_{\text{NSI}}$  due to the second line of Eq. (5). Thus we can write

$$H = H_{\text{SO}} + |\epsilon_{e\mu}^m| H_{\text{NSI}}(\epsilon_{e\mu}^m), \quad (12)$$

$$H_{\text{SO}} \equiv U_{\alpha i} \begin{pmatrix} 0 & \frac{\Delta m_{21}^2}{2E} \\ \frac{\Delta m_{21}^2}{2E} & \frac{\Delta m_{31}^2}{2E} \end{pmatrix} (U^\dagger)_{i\beta} + \begin{pmatrix} \frac{a}{2E} & 0 \\ 0 & 0 \end{pmatrix}, \quad (13)$$

$$H_{\text{NSI}}(\epsilon_{e\mu}^m) \equiv \frac{a}{2E} \begin{pmatrix} 0 & e^{i\arg[\epsilon_{e\mu}^m]} & 0 \\ e^{-i\arg[\epsilon_{e\mu}^m]} & 0 & 0 \end{pmatrix}. \quad (14)$$

Here,  $H_{\text{SO}}$  contains the standard oscillations (SO), and  $a$  is the effective matter potential, which we assume to be constant in the following. The effective NSI coupling  $\epsilon_{e\mu}^m$  is related to the parameters  $\epsilon_{e\mu}^{m\mp,f}$  from Eq. (5) by the formula

$$\epsilon_{e\mu}^m = (\epsilon_{e\mu}^{m,e+} + 3\epsilon_{e\mu}^{m,u+} + 3\epsilon_{e\mu}^{m,d+}) + (\epsilon_{e\mu}^{m,e-} + 3\epsilon_{e\mu}^{m,u-} + 3\epsilon_{e\mu}^{m,d-}). \quad (15)$$

This relation can be understood if we assume the numbers of protons, neutrons, and electrons to be the same in the Earth matter and consider only the effect of valence quarks. Furthermore, we have made use of the fact that the spin and momentum average of the Earth is zero, so that only the components of the vector interactions in the second line of Eq. (5) are relevant, and contribute equally.

In principle,  $H_{\text{NSI}}$  can also contain other non-zero entries besides  $\epsilon_{e\mu}^m$ . In combination with standard oscillations, these can lead to process chains like

$$\mu^+ \rightarrow \nu_e \xrightarrow[\text{NSI}]{\text{No osc.}} \nu_\tau \xrightarrow{\text{Osc.}} \nu_\mu \rightarrow \mu^-. \quad (16)$$

In the remainder of this section, we will neglect such contributions for conciseness, but we will exemplarily consider effects proportional to  $\epsilon_{e\tau}^m$  in our numerical analysis in Sec. 3.2. A systematic study of non-standard Hamiltonians like Eq. (14) is given in [8].

The amplitude of the flavor transition  $\nu_\alpha \rightarrow \nu_\beta$  can be calculated from the propagation Hamiltonian Eq. (12) by<sup>1</sup>

$$\langle \nu_\beta | e^{-iHL} | \nu_\alpha \rangle = (S_{\text{SO}})_{\beta\alpha} + |\epsilon_{e\mu}^m| \{S_{\text{NSI}}(\epsilon_{e\mu}^m)\}_{\beta\alpha} + \mathcal{O}(\epsilon^2). \quad (17)$$

Here, the standard oscillation amplitude  $S_{\text{SO}}$  reads

$$S_{\text{SO}} \equiv e^{-iH_{\text{SO}}L}, \quad (18)$$

and the amplitude induced by the non-standard matter effects,  $S_{\text{NSI}}$ , is given by the perturbative expansion

$$\begin{aligned} \{S_{\text{NSI}}(\epsilon_{e\mu}^m)\}_{\beta\alpha} &= \sum_{\gamma=e,\mu,\tau} (S_{\text{SO}})_{\beta\gamma} \\ &\cdot \left\{ -i \int_0^L dx e^{iH_{\text{SO}}x} H_{\text{NSI}}(\epsilon_{e\mu}^m) e^{-iH_{\text{SO}}x} \right\}_{\gamma\alpha}. \end{aligned} \quad (19)$$

In our case, the  $(e,\mu)$  and  $(\mu,e)$  elements of  $\{H_{\text{NSI}}(\epsilon_{e\mu}^m)\}_{\beta\alpha}$  are non-zero, so the golden-channel flavor transition  $\nu_e \rightarrow \nu_\mu$  can occur even in the absence of standard oscillations.

<sup>1</sup> Here we regard the NSI parameters  $\epsilon_{e\mu}^{s,m,d}$  to be small perturbations. In [26] the authors pointed out that, from the current experimental limits, the NSIs might even dominate over the oscillation effect in a  $\nu_\mu \rightarrow \nu_\tau$  oscillation experiment. In such a situation, this perturbative expansion would no longer be valid.

If, as a last step, we replace the initial and final states in Eq. (17) by the modified states from Eqs. (7) and (8), we obtain the transition probability up to first order in the  $\epsilon$  parameters as

$$P(\nu_e^{(s)} \rightarrow \nu_\mu^{(d)}) = \left| \langle \nu_\mu^{(d)} | e^{-iHL} | \nu_e^{(s)} \rangle \right|^2 \quad (20)$$

$$= |(S_{SO})_{\mu e}|^2$$

$$+ 2|\epsilon_{e\mu}^m| \text{Re} \left[ (S_{SO})_{\mu e}^* \{S_{NSI}(\epsilon_{e\mu}^m)\}_{\mu e} \right]$$

$$+ 2|\epsilon_{e\mu}^s| \text{Re} \left[ (S_{SO})_{\mu e}^* (S_{SO})_{\mu\mu} e^{i \arg[\epsilon_{e\mu}^s]} \right]$$

$$+ 2|\epsilon_{e\mu}^d| \text{Re} \left[ (S_{SO})_{\mu e}^* (S_{SO})_{ee} e^{i \arg[\epsilon_{e\mu}^d]} \right]$$

$$+ \mathcal{O}(\epsilon^2). \quad (21)$$

The zeroth order term represents the standard oscillation probability, while the first order terms contain the contributions from the different types of NSIs.

In this work, we are interested in the discovery potential for non-standard effects, i.e. in the prospects of identifying the tiny NSI contribution on the large standard oscillation background. If only the terms proportional to  $\epsilon_{e\mu}^m$  are present, this can be achieved by exploiting the different spectral structure of the signal and background events [23]. If we expand the oscillation amplitudes up to first order in  $1/E$ , we find that  $(S_{SO})_{\mu e} \sim 1/E$ , while according to Eq. (19),  $\{S_{NSI}(\epsilon_{e\mu}^m)\}_{\mu e} \sim (S_{SO})_{\mu\mu} \sim 1$ . Hence, the first (standard) term in Eq. (21) behaves as  $1/E^2$ , while the second (non-standard) term is proportional to  $1/E$ . The situation is quite different for effects proportional to  $\epsilon_{e\tau}^m$ , since for these, the non-standard terms  $\{S_{NSI}(\epsilon_{e\tau}^m)\}_{\mu e}$  will contain a factor  $(S_{SO})_{\mu\tau} \sim 1/E$ , so their lowest order energy dependence is identical to that of the standard oscillations. Therefore, the discovery reach of a neutrino factory for  $\epsilon_{e\tau}^m$  will be worse than that for  $\epsilon_{e\mu}^m$ .

For non-standard effects parameterized by  $\epsilon_{e\mu}^s$  and  $\epsilon_{e\mu}^d$ , we can read off from Eq. (21) that we are again in a favorable situation, since  $(S_{SO})_{\mu e}^* (S_{SO})_{\mu\mu} \sim 1/E$  and  $(S_{SO})_{\mu e}^* (S_{SO})_{ee} \sim 1/E$ .

### 3. DETECTING NON-STANDARD INTERACTIONS IN A NEUTRINO FACTORY

To obtain reliable estimates for the prospects of discovering non-standard interactions in a neutrino factory, we have performed detailed numerical simulations with a modified version of the GLoBES software [51, 52]. We use a neutrino factory setup based on NuFact2 from [53], with a parent muon energy of 50 GeV and a baseline of 3000 km. The total running time is 8 years (4 years in the neutrino mode, 4 years in the anti-neutrino mode), and the number of stored muons per year is  $1.066 \cdot 10^{21}$ . The detector is a 50 kt magnetized iron calorimeter, and the cross sections are based on [54, 55]. Both the wrong-sign muon appearance channel (“golden channel”) and the muon disappearance channel are taken into account.

	$\nu_e$ appearance	$\nu_\mu$ disappearance
Signal	2.5%	20%
Background	2.5%	20%

Table I: Systematical flux normalization uncertainties in our neutrino factory setup NuFact2.

We have incorporated the backgrounds due to neutral current events and muon charge misidentification.

We quantify the performance of an experiment by introducing the *discovery reach* for non-standard interactions, which is defined as the minimal magnitude of the  $\epsilon$  parameters, for which the expected experimental data is no longer consistent with a standard oscillation fit.

Following the statistical procedure described in the appendix of [53], we define the following  $\chi^2$  function <sup>2</sup>

$$\chi^2 = \min_{\lambda} \sum_j^{\text{channel}} \sum_i^{\text{bin}} \frac{|N_{ij}(\lambda^{\text{true}}, \epsilon^{\text{true}}) - N_{ij}(\lambda, \epsilon = 0)|^2}{N_{ij}(\lambda^{\text{true}}, \epsilon^{\text{true}})} + \text{Priors}, \quad (22)$$

where  $N_{ij}$  denotes the number of events in the  $i$ -th energy bin for the oscillation channel  $j$ , the vector  $\lambda = (\theta_{12}, \theta_{13}, \theta_{23}, \delta_{\text{CP}}, \Delta m_{21}^2, \Delta m_{31}^2, a, \vec{b})$  contains the standard oscillation parameters, the Mikheyev-Smirnov-Wolfenstein (MSW) potential  $a$ , and the systematical biases  $\vec{b}$ , and  $\epsilon$  represents the non-standard parameters. The index  $j$  runs over the  $\nu_e \rightarrow \nu_\mu$  and  $\nu_\mu \rightarrow \nu_\mu$  channels and over the corresponding anti-neutrino processes. For the “true” parameters used to calculate the simulated data, we adopt the following numerical values [56]:

$$\begin{aligned} \sin^2 2\theta_{12}^{\text{true}} &= 0.83, \\ \sin^2 2\theta_{23}^{\text{true}} &= 1.0, \\ \sin^2 2\theta_{13}^{\text{true}} &= 0.01, \\ (\Delta m_{21}^2)^{\text{true}} &= 8.2 \times 10^{-5} \text{ eV}^2, \\ (\Delta m_{31}^2)^{\text{true}} &= 2.5 \times 10^{-3} \text{ eV}^2. \end{aligned}$$

In the fit, we marginalize  $\chi^2$  over all standard oscillation parameters and over the systematical biases, but keep the non-standard parameters fixed at 0. The prior terms implement external input from other experiments and have the form  $(x - x^{\text{true}})^2 / \sigma_x^2$ , where  $x$  stands for any oscillation parameter or systematical bias, and  $\sigma_x$  is the corresponding externally given uncertainty. We assume  $\theta_{12}$  and  $\Delta m_{21}^2$  to be known to within 10% from solar and

<sup>2</sup> In the actual implementation, we assume the events to follow the Poisson distribution. However, for illustrative purposes, it is sufficient to consider the more compact approximative Gaussian expression.

reactor experiments [56], and include a standard deviation of 5% for the MSW potential  $a$ . All other oscillations parameters are assumed to be unconstrained since the neutrino factory itself has an excellent sensitivity to them. The systematical uncertainties are summarized in Tab. I.

For compactness, our discussion will focus on non-standard interactions induced by  $\epsilon_{e\mu}^m$ ,  $\epsilon_{e\tau}^m$ , and  $\epsilon_{e\mu}^s$ , but of course, one could also derive similar results for the other possible terms. In particular, NSIs in the detector can be expected to have similar effects to those in the source.

Furthermore, we will always assume a normal mass hierarchy, both for the simulated data and for the fit. The main influence of the inverted hierarchy is to shift the atmospheric MSW resonance to the anti-neutrino channel, which is in general less important for the overall sensitivity of the experiment because of the smaller anti-neutrino cross section. However, one can easily see that the discovery reach for non-standard interactions is robust with respect to the presence or absence of the MSW resonance: The main effect of the resonance is to enhance  $|S_{SO}|$  in Eq. (21). Therefore, if it is effective, the signal term, which is proportional to  $|S_{SO}^* S_{NSI}|$ , is enhanced. At the same time, however, also the standard oscillation background proportional to  $|S_{SO}|^2$  will become larger. These two opposing effects cancel each other, as can be seen from the  $\chi^2$  expression (22): If we assume  $\lambda^{\text{true}} = \lambda$ , the background terms drop out in the numerator, but not in the denominator. Since, however, the numerator contains an extra square, we obtain  $\chi^2 \sim |S_{SO}^* S_{NSI}|^2 / |S_{SO}|^2$ , i.e. the standard oscillation contributions cancel, and the expression is unaffected by their MSW enhancement. We have verified numerically, that our results would hardly be affected by using the inverted hierarchy for the data and the fit, even if we included parameter correlations and higher order terms.

### 3.1. Effects proportional to $\epsilon_{e\mu}^m$

We will first concentrate on non-standard effects proportional to  $\epsilon_{e\mu}^m$ , and assume all other  $\epsilon$  parameters to vanish. Fig. 2 shows the NSI discovery reach at  $3\sigma$  as a function of the true values of  $\delta_{CP}$  and  $\arg[\epsilon_{e\mu}^m]$ , and for three different values of  $|(\epsilon_{e\mu}^m)^{\text{true}}|$ . Since, according to Eq. (22),  $\arg[\epsilon_{e\mu}^m]$  and  $|\epsilon_{e\mu}^m|$  are fixed at zero in the fit, while all other parameters are marginalized over, the contours are based on the assumption of two degrees of freedom.<sup>3</sup> If the parameters lie in the white regions of the plots, non-standard interactions can be established

at the  $3\sigma$  level, while in the dark areas, the sensitivity is less than  $1\sigma$ . It is obvious that for larger  $|(\epsilon_{e\mu}^m)^{\text{true}}|$ , the white regions of good sensitivity become larger.

The characteristic band structure in Fig. 2 reveals that there are strong correlations between  $\delta_{CP}$  and  $\arg[\epsilon_{e\mu}^m]$ . To understand these correlations analytically, we note that the leading NSI signal term is proportional to  $\cos(\arg[\epsilon_{e\mu}^m] + \delta_{CP})$  [23]. Therefore, the contribution of the  $\nu_e \rightarrow \nu_\mu$  channel to the  $\chi^2$  function from Eq. (22) becomes approximately

$$\chi^2 \propto \frac{\left( \theta_{13}^{\text{true}} \cdot |(\epsilon_{e\mu}^m)^{\text{true}}| \cdot \cos(\arg[(\epsilon_{e\mu}^m)^{\text{true}}] + \delta_{CP}^{\text{true}}) \right)^2}{|(S_{SO})_{\mu e}|^2} \quad (23)$$

and is thus expected to be roughly constant along the lines of constant  $\arg[(\epsilon_{e\mu}^m)^{\text{true}}] + \delta_{CP}^{\text{true}}$ . This behavior can be nicely seen in Fig. 2.

Note that correlations do not only limit the discovery reach for non-standard interactions, but can also complicate the measurement of the standard oscillation parameters [32].

Comparing the three plots in Fig. 2, we find that for  $|(\epsilon_{e\mu}^m)^{\text{true}}| \sim 6 \cdot 10^{-4}$ , the first white islands appear, i.e. there are some parameter combinations for which the non-standard effects can be discovered at  $3\sigma$ . For  $|(\epsilon_{e\mu}^m)^{\text{true}}| \gtrsim 4 \cdot 10^{-3}$ , the  $\chi^2$  values are above  $3\sigma$  in the whole parameter space, i.e. a  $3\sigma$  discovery is always possible, independent of  $\arg[(\epsilon_{e\mu}^m)^{\text{true}}]$  and  $\delta_{CP}^{\text{true}}$ . According to Eq. (6), these numbers translate into a sensitivity to mass scales of up to  $M_{NSI} \sim 1 - 3$  TeV.

These values reappear as the top and bottom edges of the foremost (green) bars in the middle part of Fig. 3. The bars stacked below them (light blue) show how the discovery reach would improve if all standard oscillation parameters and the MSW potential were known with infinite precision, and the hindmost (blue) bars have been calculated have been calculated under the additional assumption that systematical errors are not present. The plot shows that the discovery reach depends crucially on the true values of  $\arg[\epsilon_{e\mu}^m]$  and  $\delta_{CP}$ , while systematical errors and the correlations with the fit parameters have only moderate impact.

Comparing the results for different values of  $\theta_{13}$ , we find that the achievable sensitivity for the most favorable combination of phase parameters (top edges) remains roughly unchanged as  $\theta_{13}$  decreases, while that for the most problematic parameters (bottom edges) becomes slightly better. On the one hand, smaller  $\theta_{13}$  means smaller  $(S_{SO})_{\mu e}$ , so all terms in Eq. (21) will decrease. On the other hand, the standard oscillation background, which is given by  $|(S_{SO})_{\mu e}|^2$  and therefore proportional to  $\theta_{13}^2$ , will decrease faster than the non-standard term, which is linear in  $\theta_{13}$  [23]. This makes it easier to disentangle signal and background, and especially when correlations between the standard and non-standard parameters are taken into account, this improved background suppression seems to overcompensate the smaller signal.

<sup>3</sup> One might argue that the leading term in the oscillation probability depends on the parameter combination  $\arg[\epsilon_{e\mu}^m] + \delta_{CP}$  (see Eq. (23) below), so it may be justified to use only 1 d.o.f. However, since sub-leading contributions are not completely negligible, we take 2 d.o.f. to be conservative.

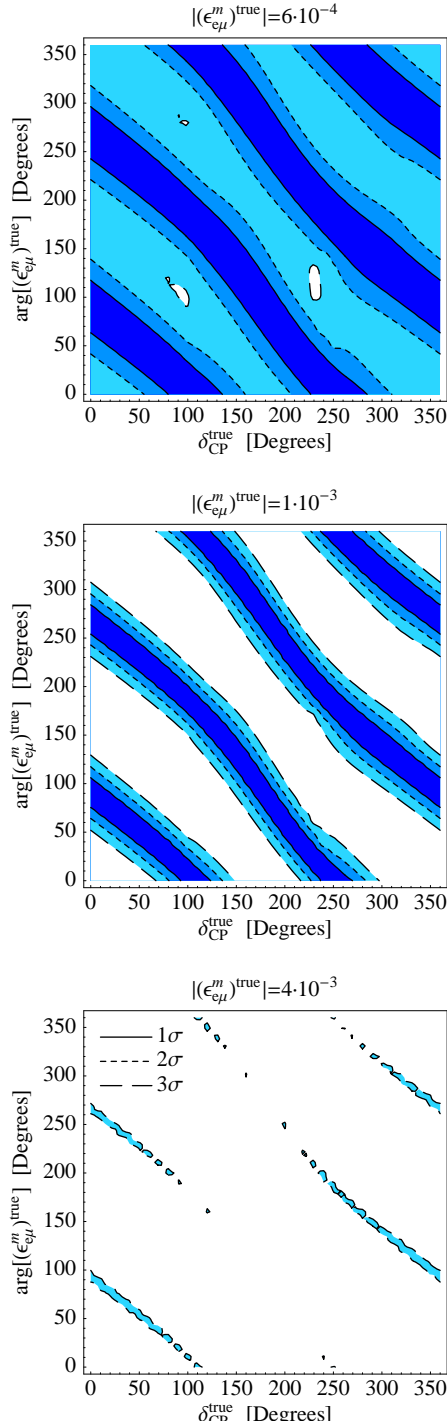


Figure 2: Contour plots of the  $\chi^2$  function defined in Eq. (22) in the  $\delta_{CP}^{\text{true}}-\arg[(\epsilon_{e\mu}^m)^{\text{true}}]$  plane for  $|\epsilon_{e\mu}^m|^{\text{true}}| = 6 \times 10^{-4}$  (top),  $1 \times 10^{-3}$  (center), and  $4 \times 10^{-3}$  (bottom). The value of  $\sin^2 2\theta_{13}$  was taken to be  $10^{-2}$  in all cases. The standard oscillation parameters and the matter potential were marginalized over.

Finally, let us compare the sensitivities predicted by our simulations with existing bounds from charged lepton flavor violating processes. In [43], Davidson et al. constrain  $|\epsilon_{e\mu}^m|$  to be smaller than  $\sim 8 \cdot 10^{-4}$  at the 90% confidence level. Assuming the respective  $\chi^2$  function to be

parabolic <sup>4</sup>, this translates into a  $3\sigma$  bound  $\lesssim 1.4 \cdot 10^{-3}$ .

---

<sup>4</sup> We are aware, that this extrapolation is problematic, since real-

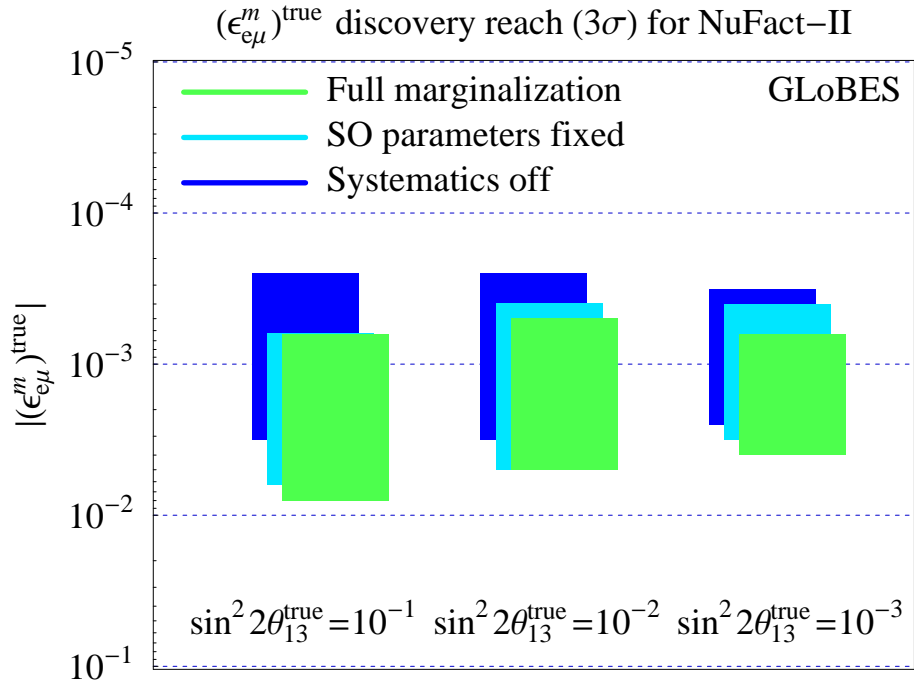


Figure 3: Limitations to the discovery reach for  $|\epsilon_{e\mu}^m|$  arising from systematical errors and from parameter correlations. The top edges of the bars indicate the values of  $|\epsilon_{e\mu}^m|$  for which there exists some combination of  $\arg[(\epsilon_{e\mu}^m)^{\text{true}}]$  and  $\delta_{\text{CP}}^{\text{true}}$ , which yields a sensitivity better than  $3\sigma$ ; the bottom edges show how large the NSIs need to be in order to be detected at this confidence level for *all* possible values of  $\arg[(\epsilon_{e\mu}^m)^{\text{true}}]$  and  $\delta_{\text{CP}}^{\text{true}}$ . The foremost (green) bars were obtained with the full analysis procedure discussed in the text, while for the intermediate (light blue) bars, the marginalization over standard oscillation parameters (including the MSW potential) was omitted, and for the hindmost (blue) bars, systematical errors were also switched off.

Comparing this number with Fig. 3, we find that part of the parameter space accessible by the neutrino factory is already ruled out, but, depending on the phase correlation, our setup may still have a significant discovery potential. This is particularly interesting if we note that the present 90% C.L. bound,  $|\epsilon_{e\mu}^m| \lesssim 8 \cdot 10^{-4}$ , comes actually from three independent bounds on the coherent forward scattering on up-quarks ( $\lesssim 8 \cdot 10^{-4}$ ), down-quarks ( $\lesssim 8 \cdot 10^{-4}$ ), and electrons ( $\lesssim 5 \cdot 10^{-4}$ ). The former two have been derived from  $\mu \rightarrow e$  conversion in nuclei, while the latter stems from the constraints on  $\mu \rightarrow 3e$ . To improve the overall bound on  $|\epsilon_{e\mu}^m|$  significantly, all three components would have to be improved. Since no experiment searching for  $\mu \rightarrow 3e$  is being designed at the moment, a neutrino factory seems to be the most realistic future option for studying  $|\epsilon_{e\mu}^m|$  in a model-independent way. Of course, if the LHC should find evidence for one specific class of models, the present bound might become much stronger already within the next few years.

istic  $\chi^2$  functions can be far from parabolic. However, it should give a useful order of magnitude estimate.

### 3.2. Effects proportional to $\epsilon_{e\tau}^m$

Let us now turn to non-standard effects proportional to  $\epsilon_{e\tau}^m$ , which are introduced in analogy to Eqs. (12) – (14). It can be read off from Fig. 4, that the sensitivity of a neutrino factory to these effects is almost two orders of magnitude worse than that to  $\epsilon_{e\mu}^m$ : Only for  $|\epsilon_{e\tau}^m| \gtrsim 3 \cdot 10^{-1}$ , discovery can be guaranteed. This can be understood from our discussion in Sec. 2, which shows that the energy dependence of standard and non-standard effects is the same, so the effect of  $\epsilon_{e\tau}^m$  can easily be absorbed into  $\lambda$ . This also explains why fixing the standard oscillation parameters improves the sensitivity by one order of magnitude.

As in the case of  $|\epsilon_{e\mu}^m|$ , the  $\theta_{13}$  dependence in Fig. 3 is weak. Actually, it could be expected to be larger here, because for the large values of  $|\epsilon_{e\tau}^m|$  required for discovery, not only the interference term between standard oscillations and NSI will contribute to the oscillation probability, but also the pure NSI term proportional to  $|\epsilon_{e\tau}^m|^2$ . For large  $\theta_{13}$ , both terms are comparable in magnitude, while for small  $\theta_{13}$ , but still large  $|\epsilon_{e\tau}^m|$ , the pure NSI term dominates. Therefore, in the latter case, the qualitative behavior of the transition probability could be expected to be simpler and thus more easily absorbed into  $\delta_{\text{CP}}$ .

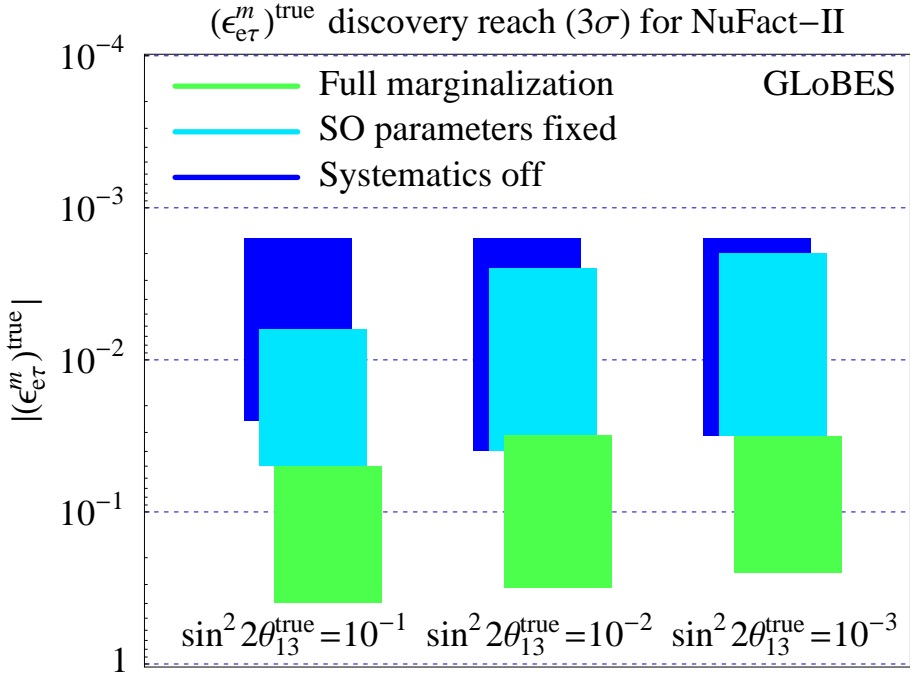


Figure 4: Limitations to the discovery reach for  $|\epsilon_{e\tau}^m|$  arising from systematical errors and from parameter correlations. The color-coding is the same as in Fig. 3.

However, we see from Fig. 4 that this effect is not very pronounced.

The present bounds on  $|\epsilon_{e\tau}^m|$  are of  $\mathcal{O}(1)$  [21, 43], so the neutrino factory could break new ground, independent of the phase correlations. Note that in [31], the authors predict an even better performance for the neutrino factory. However, they employ a completely different experimental setup with a baseline of only 732 km, and use a different analysis technique. Note also that it has been pointed out in [43, 57] that a measurement of the Weinberg angle by neutrino scattering in the near detector of a neutrino factory could improve the limit on  $|\epsilon_{e\tau}^m|$  independently to well below 0.1.

### 3.3. Effects proportional to $\epsilon_{e\mu}^s$

If the non-standard interactions do not affect neutrino oscillations, but rather the production process, we expect from Sec. 2 that the sensitivity will again be excellent because the standard and non-standard terms have different energy dependence. Indeed, Fig. 5 shows that effects with  $|\epsilon_{e\mu}^s| \sim 10^{-3}$  might be detected, and that detection can be guaranteed for  $|\epsilon_{e\mu}^s| \gtrsim 10^{-2}$ .

This discovery reach is at least one order of magnitude better than the model-independent bound of  $\mathcal{O}(10^{-1})$  coming from universality considerations in lepton decays [29]. Let us, however, remark, that present *model-dependent* bounds on  $\epsilon_{e\mu}^s$  can be already stronger than

the sensitivity of the neutrino factory.

## 4. CONCLUSIONS

We have investigated the prospects of a search for non-standard neutrino interactions in a neutrino factory experiment. We have discussed several different contributions that can arise in the effective Lagrangian, and have pointed out that these can be distinguished from the standard oscillations by their characteristic energy dependence. We have performed careful numerical simulations of a neutrino factory experiment to estimate its discovery potential for  $\epsilon_{e\mu}^m$ ,  $\epsilon_{e\tau}^m$ , and  $\epsilon_{e\mu}^s$ . It turned out that there is a strong correlation between  $\arg[\epsilon_{e\mu}^m]$  and  $\delta_{CP}$ , so that the discovery reach for  $\epsilon_{e\mu}^m$  depends strongly on the true values of these parameters: For certain combinations, a discovery of the non-standard interactions is possible for  $|\epsilon_{e\mu}^m| < 10^{-3}$ , while for less favorable scenarios,  $|\epsilon_{e\mu}^m| \sim 10^{-2}$  is required. Since the present bounds on  $|\epsilon_{e\mu}^m|$  are already of  $\mathcal{O}(10^{-3})$ , the discovery potential will crucially depend on the phase correlations. Vice-versa, however, a combination of neutrino factory results with limits from other experiments might provide additional constraints on the phases. The sensitivity to  $|\epsilon_{e\tau}^m|$  is more than one order of magnitude worse than that to  $|\epsilon_{e\mu}^m|$  due to the less favorable energy dependence of this effect. However, since present bounds on  $|\epsilon_{e\tau}^m|$  are very weak, a

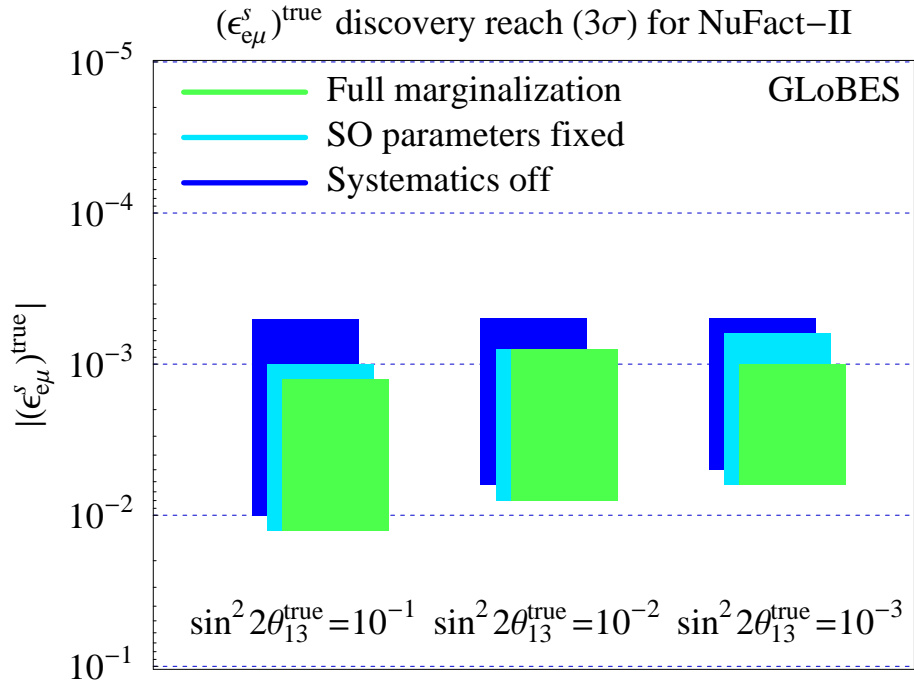


Figure 5: Limitations to the discovery reach for  $|\epsilon_{e\mu}^s|$  arising from systematical errors and from parameter correlations. The color-coding is the same as in Fig. 3.

neutrino factory could achieve a significant improvement here. Finally, the sensitivity to  $|\epsilon_{e\mu}^s|$  ranges between  $10^{-3}$  and  $10^{-2}$ , which is at least one order of magnitude better than present model-independent bounds. Thus, our simulations show that a neutrino factory is an excellent tool for detecting new physics in the neutrino sector. However, reversing the argument, this also means that possible non-standard interactions have to be taken into account when analyzing the data of such an experiment.

## Acknowledgments

We would like to thank P. Huber and W. Winter for useful discussions. This work was in part supported by the Transregio Sonderforschungsbereich TR27 “Neutrinos and Beyond” der Deutschen Forschungsgemeinschaft.

---

[1] L. Wolfenstein, Phys. Rev. **D17**, 2369 (1978).  
[2] J. W. F. Valle, Phys. Lett. **B199**, 432 (1987).  
[3] M. M. Guzzo, A. Masiero, and S. T. Petcov, Phys. Lett. **B260**, 154 (1991).  
[4] E. Roulet, Phys. Rev. **D44**, 935 (1991).  
[5] S. Bergmann, Y. Grossman, and E. Nardi, Phys. Rev. **D60**, 093008 (1999), hep-ph/9903517.  
[6] T. Hattori, T. Hasuike, and S. Wakaizumi, Prog. Theor. Phys. **114**, 439 (2005), hep-ph/0210138.  
[7] M. Garbutt and B. H. J. McKellar (2003), hep-ph/0308111.  
[8] M. Blennow, T. Ohlsson, and W. Winter (2005), hep-ph/0508175.  
[9] A. De Gouvea, G. F. Giudice, A. Strumia, and K. Tobe, Nucl. Phys. **B623**, 395 (2002), hep-ph/0107156.  
[10] T. Ota and J. Sato, Phys. Rev. **D71**, 096004 (2005), hep-ph/0502124.  
[11] Y. Grossman, Phys. Lett. **B359**, 141 (1995), hep-ph/9507344.  
[12] S. Bergmann, M. M. Guzzo, P. C. de Holanda, P. I. Krastev, and H. Nunokawa, Phys. Rev. **D62**, 073001 (2000), hep-ph/0004049.  
[13] Z. Berezhiani, R. S. Raghavan, and A. Rossi, Nucl. Phys. **B638**, 62 (2002), hep-ph/0111138.  
[14] A. Friedland, C. Lunardini, and C. Pena-Garay, Phys. Lett. **B594**, 347 (2004), hep-ph/0402266.  
[15] O. G. Miranda, M. A. Tortola, and J. W. F. Valle, JHEP **10**, 008 (2006), hep-ph/0406280.  
[16] M. C. Gonzalez-Garcia *et al.*, Phys. Rev. Lett. **82**, 3202 (1999), hep-ph/9809531.  
[17] S. Bergmann, Y. Grossman, and D. M. Pierce, Phys. Rev. **D61**, 053005 (2000), hep-ph/9909390.  
[18] N. Fornengo, M. Maltoni, R. T. Bayo, and J. W. F. Valle, Phys. Rev. **D65**, 013010 (2002), hep-ph/0108043.

- [19] M. C. Gonzalez-Garcia and M. Maltoni, Phys. Rev. **D70**, 033010 (2004), hep-ph/0404085.
- [20] A. Friedland, C. Lunardini, and M. Maltoni, Phys. Rev. **D70**, 111301 (2004), hep-ph/0408264.
- [21] A. Friedland and C. Lunardini, Phys. Rev. **D72**, 053009 (2005), hep-ph/0506143.
- [22] S. Bergmann and Y. Grossman, Phys. Rev. **D59**, 093005 (1999), hep-ph/9809524.
- [23] T. Ota, J. Sato, and N.-a. Yamashita, Phys. Rev. **D65**, 093015 (2002), hep-ph/0112329.
- [24] T. Ota and J. Sato, Phys. Lett. **B545**, 367 (2002), hep-ph/0202145.
- [25] M. Honda, N. Okamura, and T. Takeuchi (2006), hep-ph/0603268.
- [26] N. Kitazawa, H. Sugiyama, and O. Yasuda (2006), hep-ph/0606013.
- [27] A. Friedland and C. Lunardini, Phys. Rev. **D74**, 033012 (2006), hep-ph/0606101.
- [28] M. Blennow, T. Ohlsson, and J. Skrotzki (2007), hep-ph/0702059.
- [29] M. C. Gonzalez-Garcia, Y. Grossman, A. Gusso, and Y. Nir, Phys. Rev. **D64**, 096006 (2001), hep-ph/0105159.
- [30] P. Huber and J. W. F. Valle, Phys. Lett. **B523**, 151 (2001), hep-ph/0108193.
- [31] A. M. Gago, M. M. Guzzo, H. Nunokawa, W. J. C. Teves, and R. Zukanovich Funchal, Phys. Rev. **D64**, 073003 (2001), hep-ph/0105196.
- [32] P. Huber, T. Schwetz, and J. W. F. Valle, Phys. Rev. **D66**, 013006 (2002), hep-ph/0202048.
- [33] M. Campanelli and A. Romanino, Phys. Rev. **D66**, 113001 (2002), hep-ph/0207350.
- [34] A. Bueno, M. Campanelli, M. Laveder, J. Rico, and A. Rubbia, JHEP **06**, 032 (2001), hep-ph/0010308.
- [35] R. Adhikari, S. K. Agarwalla, and A. Raychaudhuri, Phys. Lett. **B642**, 111 (2006), hep-ph/0608034.
- [36] G. L. Fogli, E. Lisi, A. Mirizzi, and D. Montanino, Phys. Rev. **D66**, 013009 (2002), hep-ph/0202269.
- [37] H. Duan, G. M. Fuller, J. Carlson, and Y.-Z. Qian (2006), astro-ph/0608050.
- [38] G. Mangano *et al.*, Nucl. Phys. **B756**, 100 (2006), hep-ph/0607267.
- [39] Z. Berezhiani and A. Rossi, Phys. Lett. **B535**, 207 (2002), hep-ph/0111137.
- [40] J. Barranco, O. G. Miranda, C. A. Moura, and J. W. F. Valle, Phys. Rev. **D73**, 113001 (2006), hep-ph/0512195.
- [41] J. Barranco, O. G. Miranda, and T. I. Rashba, JHEP **12**, 021 (2005), hep-ph/0508299.
- [42] J. Barranco, O. G. Miranda, and T. I. Rashba (2007), hep-ph/0702175.
- [43] S. Davidson, C. Pena-Garay, N. Rius, and A. Santamaria, JHEP **03**, 011 (2003), hep-ph/0302093.
- [44] S. Geer, Phys. Rev. **D57**, 6989 (1998), hep-ph/9712290.
- [45] C. Albright *et al.* (2000), hep-ex/0008064.
- [46] M. Apollonio *et al.* (2002), hep-ph/0210192.
- [47] P. Huber, M. Lindner, M. Rolinec, and W. Winter, Phys. Rev. **D74**, 073003 (2006), hep-ph/0606119.
- [48] P. Huber, T. Schwetz, and J. W. F. Valle, Phys. Rev. Lett. **88**, 101804 (2002), hep-ph/0111224.
- [49] M. Freund, P. Huber, and M. Lindner, Nucl. Phys. **B615**, 331 (2001), hep-ph/0105071.
- [50] M. Freund, P. Huber, and M. Lindner, Nucl. Phys. **B585**, 105 (2000), hep-ph/0004085.
- [51] P. Huber, M. Lindner, and W. Winter, Comput. Phys. Commun. **167**, 195 (2005), <http://www.ph.tum.de/~globes>, hep-ph/0407333.
- [52] P. Huber, J. Kopp, M. Lindner, M. Rolinec, and W. Winter (2007), hep-ph/0701187.
- [53] P. Huber, M. Lindner, and W. Winter, Nucl. Phys. **B645**, 3 (2002), hep-ph/0204352.
- [54] M. D. Messier, *Evidence for neutrino mass from observations of atmospheric neutrinos with Super-Kamiokande*, Ph.D. thesis, Boston University (1999), uMI-99-23965.
- [55] E. A. Paschos and J. Y. Yu, Phys. Rev. **D65**, 033002 (2002), hep-ph/0107261.
- [56] M. Maltoni, T. Schwetz, M. A. Tortola, and J. W. F. Valle, New J. Phys. **6**, 122 (2004), hep-ph/0405172.
- [57] M. L. Mangano *et al.* (2001), hep-ph/0105155.